Site-selective Synthesis of 1,3-Dioxin-3-ones via a Gold(I) Catalyzed Cascade Reaction

Site-selective Synthesis of 1,3-Dioxin-3-ones via a Gold(I) Catalyzed Cascade Reaction

Juzeng An,[a†] Riccardo Pedrazzani,[a] Magda Monari,[a] Marta Marin-Luna,[b†] Carlos Silva Lopez,[b,c*] Marco Bandini[a]

ABSTRACT: A novel gold(I)-catalyzed protocol for the synthesis of 4H-1,3-dioxin-3-ones is presented. The protocol exploits a metal induced cascade sequence involving a [3,3]-sigmatropic rearrangement followed by regioselective O-annulation reactions. A wide range of oxygen-based heterocyclic scaffolds (21 examples) were achieved in excellent yield (up to 80%) and a detailed computation as well as deuterium-labelling investigations enabled all the plausible reaction pathways to be mapped and the rationalization of the recorded regioselectivity.

Homogenous gold catalysis has revolutionized the realm of the manipulation of unsaturated unfunctionalized hydrocarbons in just twenty years.1 In particular, the site-selective electrophilic activation of C-C double and triple bonds enabled a plethora of single- as well as multi-step synthetic sequences in a convenient manner.

The synthesis of densely functionalized heterocycles deeply benefited by this advent, exploiting the unique functional groups tolerance exerted by cationic [Au(I)] complexes and the realization of new C-C and C-X annulation events.2 In this context, the 1,3-dioxin-3-one scaffold (A, Figure 1a) is of particular relevance since it identifies synthetically flexible building blocks for organic transformations such as: ketene chemistry, aromatization reactions, rearrangements, cycloadditions and total syntheses.3 In addition, aromatic analogous of the 1,3-dioxin-3-one scaffolds (Figure 1b), namely dioxanones4 are common motifs in numerous natural compounds (i.e. chlorotheolide family) that display intense antiproliferative actions on several tumor cell lines.5

Notably, despite the undoubted transversal utility of this class of building blocks, their preparation still relies on stoichiometric protocols (i.e. lithiation/alkylation, [4+2]-cycloadditions) with only few notable catalytic exceptions.[6] Therefore, the request for flexible, selective and environmentally benign synthetic methodologies for their preparation has been and continues to be widely investigated.

In continuation with our ongoing commitment towards the realization of gold catalyzed electrophilic activations of alkynes,7,8 we envisioned the possibility to realize a new direct synthetic protocol of densely functionalized 1,3-dioxin-3-ones via [Au(I)]-assisted manipulation of readily available propargylic-ketoesters 1. In particular, an initial intramolecular [3,3]-sigmatropic rearrangement9 could lead to the corresponding carboxyallene intermediate 1' that might undergo a rapid annulation reaction delivering the desired six-membered ring 2 (Figure 1c). However, the present working plan poses several important regiochemical interrogatives due to the multiple electrophilic as well as nucleophilic sites present in the **[Au+]-1** adduct.

Figure 1. a) The 1,3-dioxin-3-one scaffold (**A**) and relative synthetic manipulations; b) a representative example of natural occurring compound comprising the dioxanones core; c) the present gold(I)-catalyzed synthetic approach to **2**.

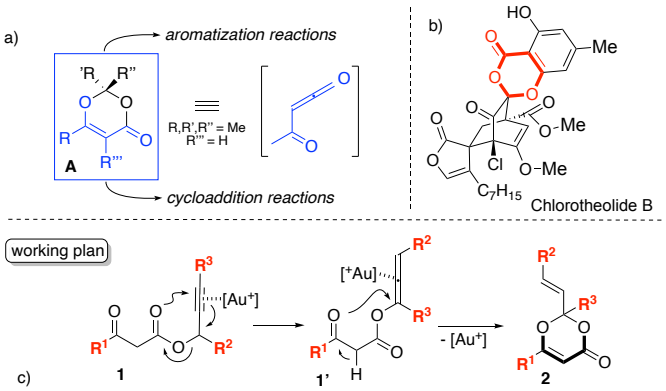

Aiming to verify our hypothesis and to get optimal reaction conditions, an extensive survey of reaction parameters was carried out by considering the propargylate 1a as a model substrate. In Table 1, a summary of tested reaction parameters is reported (see SI for a complete collection of results).

Delightly, we found out that JohnPhosAuNTf2 (5 mol%) proved to be the catalyst of election over a series of phosphine and carbene-based gold complexes (C2-C10). Additionally, the use of

Table 1. Optimization of the reaction conditions

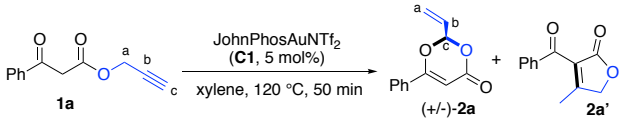

$PPh_3AuCl/AgNTf_2$ (**C2**)
JackiePhosAuCl/$AgNTf_2$ (**C3**)
XPhosAuCl/$AgNTf_2$ (**C4**)
$CH_2(PPh_2AuCl)_2/AgNTf_2$ (**C5**)
dppe$(AuCl)_2/AgNTf_2$ (**C6**)
biphep$(AuCl)_2/AgNTf_2$ (**C7**)

Xantaphos$(AuCl)_2/AgNTf_2$ (**C8**)
IPrAuCl/$AgNTf_2$ (**C9**)

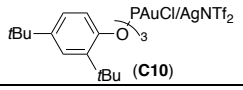

Run[a]	Deviation from optimal	Yield **2a**/**2a'** (%)[b]
1	--	80
2	**C1** at 60 °C, toluene	50/-
3	**C2** at 60 °C, toluene	22/-
4	**C3** at 60 °C, toluene	42/-
5	**C4** at 60 °C, toluene	40/-
6	**C5** at 60 °C, toluene	NR
7	**C6** at 60 °C, toluene	20/19
8	**C7** at 60 °C, toluene	13/-
9	**C8** at 60 °C, toluene	-/25
10	**C9** at 60 °C, toluene	20/-
11	**C10** at 60 °C, toluene	NR
12[c]	$AgSbF_6$ instead of $AgNTf_2$	37/-
13[c]	AgTFA instead of $AgNTf_2$	NR
14[c]	AgOTf instead of $AgNTf_2$	37/9
15	with KOAc (2 eq)	40/-
16	Toluene 100 °C	60/-
17	Toluene 120 °C	68

Reaction conditions: **1a** (0.2 mmol, 0.05 M), under nitrogen conditions. [b] Determined after flash chromatography. [c] The cationic gold complex was obtained in situ in toluene. NR: no reaction.

reagent grade xylene at 120 °C and very short reaction time (50 min) fulfilled the optimal parameters delivering the dioxinone 2a in high regiochemical manner and 80% yield (Scheme in Table 1).

Worthy of mentioning, the protocol led almost exclusively to the six-membered scaffold through the planned O-ring-closing procedure. On the contrary, the five-membered counterpart 2a' was observed in very low amount mainly when bidendate phosphines were employed (entries 6-9). Analogously, NTf2- emerged as the counterion of election among the ones tested (entry 1 vs entries 12-14).10 Finally, while the addition of a base (i.e. KOAc) did not affect significantly the final outcome of the process (entry 15), an increase in the temperature (entries 16 and 17) led to a significant improvement in the isolation of 2a (up to 68% in toluene at 120 °C).

Having established the optimal parameters with compound 1a, the generality of the protocol was envisioned by reacting, under the conditions reported in the Scheme of Table 1, a series of terminal propargylic derivatives carrying molecular variations on the □-ketoester motif (1b-p). The corresponding chemical outcomes have been collected in the Scheme 1. Ketoesters featuring diversely functionalized aromatic rings at the keto-site were adequately tolerated regardless the electronic properties of the substituents. In details, sterically congested ortho-substituted arenes (i.e. 2b, 2d and 2k) and the mesitylene analogous 2e performed satisfyingly too, delivering the corresponding dioxin-3-one cores in good yields (up to 72%).

Scheme 1. Scope of the reaction. Variations on the □-ketoester skeleton (X-ray structure of 2k is also documented).

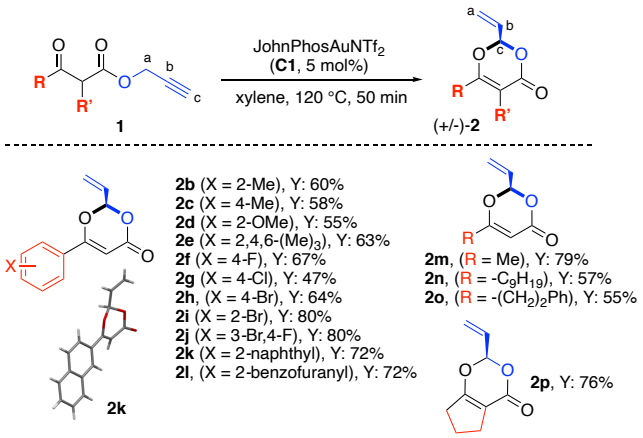

Analogously, when electron-donating (1b-e, 1k and 1l) or electron-withdrawing (1f-j) units were accommodated at the aromatic acyclic precursor, excellent catalytic performance were recorded (yield up to 80%). Linear and cyclic aliphatic ketones were also synthesized and tested under optimal conditions (1m-p). Interestingly, no variations on the final outcome were recorded in all cases (yields: 55-79%).

Then, our focus moved on the applicability of the protocol towards precursors carrying structural diversity at the propargylic unit. In this line, a series of acyclic precursors comprising internal alkynes and branched side chains (1q-u) were subjected to optimal reaction conditions.

The data collected in Scheme 2 contributed to emphasize the generality of the method. Here, propargylic carboxylates deriving from primary and secondary alcohols guaranteed satisfactory results in the cyclization reactions along with high stereospecificity for the newly formed C=C bond. Analogously, the internal alkyne 1t worked satisfyingly in the cascade process delivering the

corresponding dioxin-3-one scaffold 2t in 62% yield.

Scheme 2. Scope of the reaction. Variations on the propargylic chain.

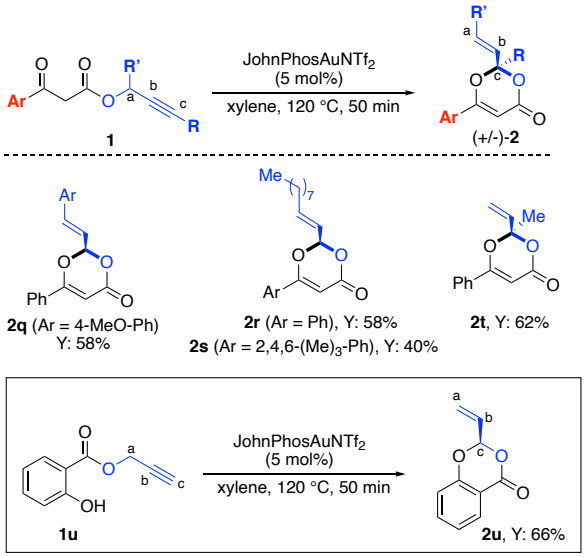

Finally, the possibility to apply the present methodology towards the realization of vinyl-dioxanones was envisioned and successfully realized by subjecting the carboxylate 1u to optimal conditions. Satisfyingly, the corresponding vinyl derivative 2u was obtained in 66% yield and high chemoselective manner.

Prompted by the experimental evidences and intrigued by the mostly selective isolation of 2a, we performed a computational study on the mechanism governing the trans-formation of 1a into 2a and 2a' through DFT. We chose the OTf- (i.e. X in Scheme 3) anion as counterion as both isomers 2a/2a' are isolated experimentally when it is present; a summary of the proposed mechanism is depicted in Scheme 3a (for a full mechanism see the SI). An analysis of the thermochemical stability of both alternate products, 2a and 2a', suggests that the C-cyclized isomer 2a', is substantially lower in energy than the experimentally observed 2a, thereby revealing that the 1a → 2a conversion should be kinetically controlled. Initially, the gold complex coordinates to the alkynyl moiety of the keto-enol tautomer of 1, which is more stable thermodynamically, forming intermediate INT0 (+12.0 kcal•mol-1). The subsequent stepwise [3,3]-sigmatropic rearrangement process towards INT211 involves a stretched 1,3-dioxane-like gold complex featuring an allene fragment, INT1. This intermediate is strikingly more stable than both ends of the sigmatropic process by about 6 kcal•mol-1. Once INT2 is formed two pathways could be drawn depending on its O- or C-annulation mode leading respectively to a 1,3-dioxin-3-one specie INT3-A and to an unsaturated lactone derivative INT3-B. Computational results revealed that TS3-A, concerning a simultaneously O-cyclization and proton trapping by the OTf anion, is +2.9 kcal•mol-1 lower in energy than the alternative C-cyclized transition state TS3-B. This energetic difference would be enough to observe product selectivity (2a vs 2a'). A posterior barrierless protodeauration process at INT3-A affords the dioxinone derivative 2a (ΔGTS4-A = -1.6 kcal•mol-1) whereas the similar event at INT3-B, to lead the five-membered isomer 2a', implies at higher energetic cost ($\Delta G^{\neq}$ TS4-B = +13.1 kcal• mol-1).12

On the other hand, deuterium-labeling experiments carried out on 1a-d3 (see SI for details) revealed a substantial incorporation of D-atom (51%) at the internal vinyl position (Cb) of product

2, supporting for the protodeauration of the alkenyl-gold intermediate INT3-A as the latest stage of the catalytic cycle. Analogously, the high deuteration content at the acetal position Cc prompted us to exclude an Au-acetylide mediated cyclization mechanism (Scheme 3b).13 Partial deuteration of the Ca-position (ca. 42%) prompted us to consider the participation of a propargylate/allenoate equilibria of INT0. Our calculations however revealed that this intermediate is very unstable (18 kcal mol-1) and is therefore unlikely to participate in this chemistry. Another viable alternative that explain this partial deuteration is a 1,3-H shift at INT1 (most probably stepwise, intermolecular and counterion-mediated).

Scheme 3. Computed mechanism for the transformation of **1** into **2** and **2a'** at the PCM(*p*-Xylene)/M06/def2-SVP theoretical level. Gibbs free energies are reported in kcal mol^{-1} (1 atm and 298 K), relative to keto-enol tautomer of **1a**. L refers to PMe_3 and X to OTf anion.

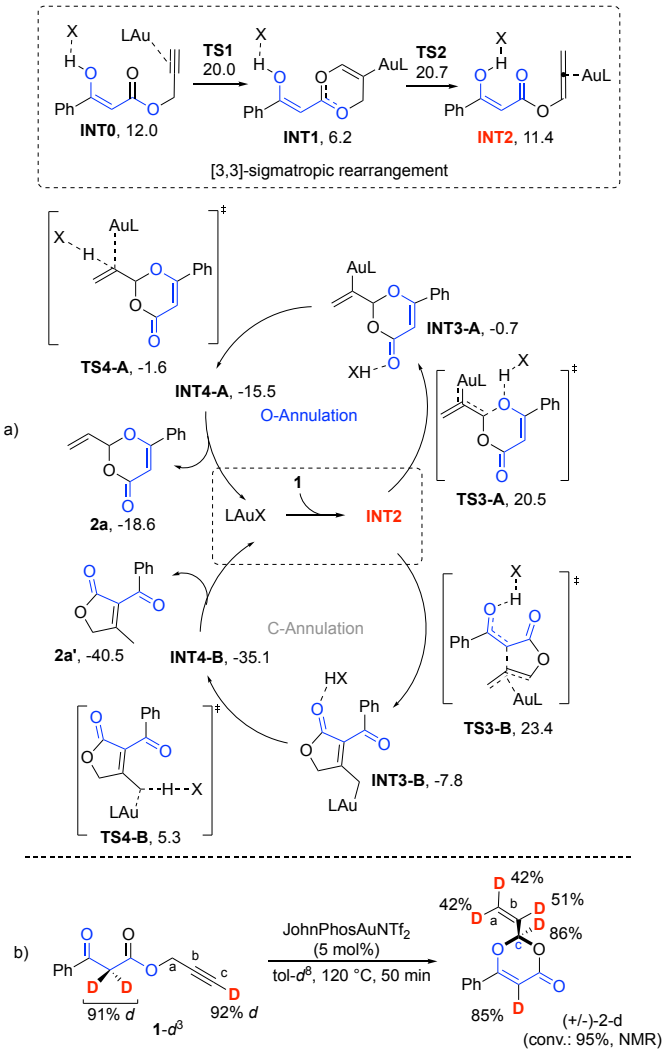

In conclusion, a novel gold catalyzed synthetic methodology for a rapid access to densely functionalized dioxinones (yield up to 80%) is documented. The protocol exploits the attitude of homogeneous gold(I) catalysis to assist multiple and consecutive chemical events (i.e. sigmatropic rearrangement/nucleophilic trapping of allenes) via site-selective electrophilic activation of π-systems. The high degree of regioselectivity recorded was corroborated via a detailed computational investigation that also mapped all key intermediates of the dual gold activation mode exerted during the catalytic cycle.

Conflicts of interest

There are no conflicts to declare.

Notes and references

The Supporting Information is available free of charge on the ACS Publications website. Experimental procedures and analytical characterization of unknown compounds (PDF); NMR-Spectra (PDF); Computational data and Cartesian coordinates (PDF); CIF file for 2k X-ray (.cif)

AUTHOR INFORMATION

Corresponding Author

* MB: marco.bandini@unibo.it.

* CSL: carlos.silva@uvigo.es

Present Addresses:

† J.A. Institute of Chemical Research of Catalonia (ICIQ), The Barcelona Institute of Science and Technology, Av. Països Catalans 16, 43007 Tarragona, Spain.

MM-L: Departamento de Química Orgánica, Facultad de Química, Regional Campus of International Excellence ‘‘Campus Mare Nostrum’’, Universidad de Murcia, Murcia-30100, Spain.

ACKNOWLEDGMENT

J.A. is grateful to CSC Programme No. 201608310110. University of Bologna is acknowledged for financial support. C.S.L and M.M. are grateful to CESGA for allocation of HPC resources and to MICINN (CTQ2016-75023-C2-2-P) and Xunta de Galicia (ED431E 2018/07) for funding.

REFERENCES

1 (a) A. S. K. Hashmi, *Acc. Chem. Res.,* 2014, **47**, 864; (b) L. Zhang, *Acc. Chem. Res.,* 2014, **47**, 877; (c) A. Fürstner, *Acc. Chem. Res.,* 2014, **47**, 925; (d) C. Obradors, A. M. Echavarren, *Chem. Commun.,* 2014, **50**, 16; (e) J. Xie, C. Pan, A. Abdukader, C. Zhu, *Chem. Soc. Rev.,* 2014, **43**, 5245; (f) D. Qian, J. Zhang, *Chem. Soc. Rev.,* 2015, **44**, 677; (h) Y. Wang, M. E. Muratore, A. M. Echavarren, *Chem. Eur. J.,* 2015, **21**, 7332; (g) M. Joost, A. Amgoune, D. Bourissou, *Angew. Chem. Int. Ed.,* 2015, **54**, 15022; (h) S. Kramer, *Chem. Eur. J.,* 2016, **22**, 15584; (j) L. Liu, *J.* Zhang, *Chem. Soc. Rev.,* 2016, **45**, 506; (k) W. Zi, F. D. Toste, *Chem. Soc. Rev.,* 2016, **45**, 4567; (l) A. Nijamudheen, A. Datta, *Chem. Eur. J.,* 2020, **26**, 1442.

2 (a) N. Krause, C. Winter, *Chem. Rev.,* 2011, **111**, 1994; (b) H. Huang, Y. Zhou, H. Liu, Beilstein *J. Org. Chem.,* 2011, **7**, 897; (c) H.C. Shen, T.H. Graham, *Drug Discovery Today,* 2013, **10**, 33; (d) M. Petrovic, E. G. Occhiato, *Chem. Eur. J.,* 2016, **11**, 642; (e) F. Pan, C. Shu. L. W. Ye, *Org. Biomol. Chem.,* 2016, **14**, 9456; (f) M. Bandini in *Au-Catalyzed Synthesis and Functionalization of Heterocycles*, *Top. Heterocyclic Chem.* Springer, 2016; (g) F. Pan, C. Shu, L. W. Ye, *Org. Biomol. Chem.,* 2016, **14**, 9456; (h) Y. C. Lee, K. Kumar, *Isr. J. Chem.,* 2018, **58**, 531; (i) D. Pflästerer, M. Rudolph, A. S. K. Hashmi, *Isr. J. Chem.,* 2018, **58**, 622; (j) N. Kaur, *Synth. Commun.,* 2019, **49**, 1459; (k) N. Kaur, P. Bhardwaj, M. Devi, Y. Vermal, P. Grewal, *SN App. Science,* 2019, **1**, 903.

3 For representative examples see: (a) R. J. Clemens, J. A. Hyatt, *J. Org. Chem.,* 1985, **50**, 2431; (b) Y. Hatsui, K. Li, A. Mori, H. Takeshita, *Heterocycles,* 2001, **54**, 765; (c) I. Navarro, J. F. Basset, S. Habbe, S. M. Major, T. Wener, C. Howsham, J. Brackow, A.G.M. Barrett, *J. Am. Chem. Soc.,* 2008, **130**, 10293; (d) P. S. Blencowe, A. G. M. Barrett, *Can. J. Chem.,* 2012, **90**, 975; (e) M. Seyyedhamzeh, *Synlett,* 2012, **23**, 1556; (f) J. Zhang, J. Xu, *Helv. Chim. Acta*, 2013, **96**, 1733; (g) Q. Xiao, K. Young, A. Zakarian, *Org. Lett.,* 2013, **15**, 3314; (h) P.S. Blencowe, A.G.M. Barrett, *Eur. J. Org.,* 2014, 22 4844; (i) S.N. Karad, W.K. Chung, R. S. Liu, *Chem. Sci.,* 2015, **6**, 5964; (j) S.N. Karad, W. K. Chung, R. S. Liu, *Chem.Commun.,* 2015, **51**, 13004; (k) D.V. Severnard, A.V. Didenko, D. Lorenz, M. Vorobiev, J. Stelten, T. Dülcks, V.S. Sosnovskikh, *Tetrahedron,* 2017, **73**, 1495; (l) R. Galaverna, T. McBride, J. C. Pastre, D.L. Browne, *React. Chem. Eng.,* 2019, **4**, 1559; (m) G. Marsico, M. S. Ciccone, M. Masi, F. Freda, M. Cristofaro, A. Evidente, S. Superchi, P. Scafato, *Molecules*, 2019, **24**, 3193; (n) T. K. Ma, P. J. Parsons, A. G. M. Barrett, *Eur. J. Org. Chem.,* 2020, 1, 28; (p) K. L. Mendhekar, T. R. Pradhan, D. K. Mohapatra, *J. Org. Chem.,* 2020, **85**, 4881.

4 For a Pd-catalyzed complementary approach to vinyl-dioxanones see: Y. Ogiwara, K. Sato, N. Sakai, *Org. Lett.,* 2017, **19**, 5296. See also: D. C. Elliott, T. K. Ma, A. Selmani, R. Cookson, Parsons, A. G. M. Barret, *Org. Lett.,* 2016, **18**, 1800.

5 L. Liu, Y. Han, J. Xiao, L. Li, L. Guo, X. Jiang, L. Kong, Y. Che, *J. Nat. Prod.,* 2016, **79**, 2616.

6 (a) M. Sato, K. Sekiguchi, H. Ogasawara, C. Kaneko, *Synthesis*, 1985, **2**, 224; (b) M. Sato, H. Ogasawara, K. Oi, T. Kato, *Chem. Pharm. Bull.,* 1983, **31**, 1896; (c) M. Sato, N. Yoneda, C. Kaneko, *Chem. Pharm. Bull.,* 1986, **34**, 621; (d) M. Murakami, H. Kamaya, C. Kaneko, M. Sato, *Tetrahedron Asymm.,* 2003, **14**, 201; (e) A. R. Katritzky, Z. Wang, M. Wang, C. D. Hall, K. Suzuki, *J. Org. Chem.,* 2005, **70**, 4854; (f) M. S. Wang, Z. Wang, W. Chen, X. Yang, H. Zhang, *Org. Lett.,* 2019, **21**, 1881.

7 (a) G. Cera, P. Crispino, M. Monari, M. Bandini, *Chem. Commun.,* 2011, **47**, 7803; (b) G. Cera, S. Piscitelli, M. Chiarucci, G. Fabrizi, A. Goggiamani, R. S. Ramón, S. P. Nolan, M. Bandini, *Angew. Chem. In. Ed.,* 2012, **51**, 9891; (c) G. Cera, M. Chiarucci, A. Mazzanti, M. Mancinelli, M. Bandini, *Org. Lett.,* 2012, **14**, 1350; (d) M. Chiarucci, R. Mocci, L. D. Syntrivanis, G. Cera, A. Mazzanti, M. Bandini, *Angew. Chem. Int. Ed.,* 2013, **52**, 10850; (e) M. Chiarucci, E. Matteucci, G. Cera, G. Fabrizi, M. Bandini, *Chem. Asian J.,* 2013, **8**, 1776; (f) G. Cera, M. Chiarucci, F. Dosi, M. Bandini, *Adv. Synth. Catal.,* 2013, **355**, 2227; (g) P. Giacinto, G. Cera, A. Bottoni, M. Bandini, G. P. Miscione, *ChemCatChem,* 2015, **7**, 2480; (h) M.M. Mastandrea, N. Mellonei, P. Giacinto, A. Collado, S. P. Nolan, G. P. Miscione, A. Bottoni, M. Bandini, *Angew. Chem. Int. Ed.,* 2015, **54**, 14885; (i) E. Manoni, M. Daka, M. M. Mastandrea, A. De Nisi, M. Monari, M. Bandini, *Adv. Synth. Catal.,* 2016, **358**, 1404; (l) A. De Nisi, C. Bergamini, M. Leonzio, G. Sartor, R. Fato, M. Monari, N. Calonghi, M. Bandini, *Dalton Transactions,* 2016, **45**, 1546; (m) M. Bandini, G. Cera, G. P. Miscione, *ChemCatChem,* 2017, **9**, 316; (n) J. An, A. Parodi, M. Monari, M. Castiñeira Reis, C. Silva Lopez, M. Bandini, *Chem. Eur. J.,* 2017, **23**, 2442.

8 For general review see: (a) M. E. Muratore, A. Homs, C. Obradors, A. M. Echavarren, *Chem. Asian J.,* 2014, **9**, 3066; (b) R. Dorel, A. M. Echavarren, *Chem. Rev.,* 2015, **115**, 9028; (c) W. Debrouwer, T. S. A. Heugebaert, B. I. Roman, C. V. Stevens, *Adv. Synth. Catal.,* 2015, **357**, 2975; (d) A. M. Asiri, A. S. K. Hashmi, *Chem. Soc. Rev.,* 2016, **45**, 4471; (e) B. Zhang, T. Wang, Asian *J. Org. Chem.,* 2018, **7**, 1758.

9 (a) N. Marion, S.P. Nolan, *Angew. Chem. Int. Ed.,* 2007, **46**, 2750; (b) S. Wang, G. Zhang, L. Zhang, *Synlett,* 2010, **5**, 692; (c) R. K. Shiroodi, Gevorgyan, *Chem. Soc. Rev.,* 2013, **42**, 4991; (d) C. Obradors, A. M. Echavarren, *Acc. Chem. Res.,* 2014, **47**, 902.

10 For general reviews on the topic see: (a) M. Jia, M. Bandini, *ACS Catalysis,* 2015, **5**, 1638; (b) B. Ranieri, I. Escofet, A. E. Echavarren, *Org. Biomol. Chem.,* 2015, **13**, 7103; (c) J. Schießl, J. Schulmeister, A. Doppiu, E. Wörner, M. Rudolph, R. Karch, A. S. K. Hashmi, *Adv. Synth. Catal.,* 2018, **360**, 2493.

11 The selective formation of the dioxinone **2t**, featuring a quaternary stereogenic center, supports the initial gold catalyzed [3,3]-sigmatropic event.

12 Protodeauration barriers, showing a strong substrate dependency, can range from kinetically irrelevant to rate limiting steps. See for instance (a) R. B. Ahmadi, P. Ghanbari, N.A. Rajabi, A.S.K. Hashmi, B. F. Yates, A. Ariafard., Organometallics, 2015, **34**, 3186; (b) I. Stylyanakis, O. N. Faza, O.; C. S. Lopez, A. Kolocouris A., *Org. Chem. Front*. *Org. Chem. Front*. 2020, **7**, 997.

13 The presence of adventitious traces of water in the reaction media could address for the partial loss of deauration content in **2a**-**d**.